

Space-Time Recovery of Arbitrarily Shaped Wave-Packets by Means of Three Dimensional Imaging Technique

A. Matijošius¹, R. Piskarskas¹, E. Gaižauskas¹, A. Dubietis¹, P. Di Trapani²

¹Department of Quantum Electronics, Vilnius University
Saulėtekio av. 9, bldg. 3, LT-10222 Vilnius, Lithuania

²Istituto Nazionale di Fisica della Materia (INFM) and
Department of Physics, University of Insubria, Via Valleggio 11, IT-22100 Como, Italy

Received: 22.04.2004

Accepted: 05.07.2004

Abstract. We study numerically and experimentally self-focusing dynamics of femtosecond light pulses. By demonstrating the potential of three dimensional imaging technique for quantitative recovery of complex (arbitrarily shaped) wave packets, we monitor space-time transformation dynamics of 150-fs light pulse, which undergoes self-focusing and filamentation in water. Peculiar spatio-temporal and spectral features reveal conical nature of resulting wave-packet.

Keywords: self-focusing, light filament, space-time focusing.

1 Introduction

Spatial and temporal transformations of wave packets which undergo self-focusing in transparent media with Kerr nonlinearity attract a great deal of interest from the point of view both of fundamental and applied science. Self-focusing of ultrashort light pulses with power well exceeding that for continuous-wave beam collapse gives rise to a variety of spatial, temporal and interrelated (spatio-temporal, ST) effects and has been a topic of intense theoretical and experimental research; for a comprehensive review, see [1] and references therein. Discovery of a spontaneous filament formation accompanying intense femtosecond pulse propagation in air [2] boosted an interest in ST transformation through filamentation dynamics in

gasses [3, 4], solids [5] and liquids [6, 7] under a common concept of White Light Laser [8].

Numerical models of different dimensionality and complexity have been elaborated to study temporal, and, more generally, ST dynamics. Propagation of intense light pulses in media with rather distinct optical properties (amount of normal group-velocity dispersion, nonlinearity, etc; namely gasses, solids and liquids) under various initial conditions (pulse duration, beam width, power, wavelength) has been examined. In spite of different regimes investigated, temporal pulse splitting emerged as a common feature resulting from the interplay between self-focusing, self-phase-modulation and normal dispersion, see [9] and references therein. Along with temporal features, rich space-time dynamics is expected, therefore experimental confirmation of the numerical results is a primary concern in understanding the underlying physics.

The major problem related to experimental characterization of the wave packet dynamics is that most of the measurements had been limited either to pure temporal domain, by standard on-axis auto or cross correlation technique, or to the pure spatial one, by time-integrated CCD-based detection. Although these techniques provide useful information on pulse or beam characteristics, and could be extended by incorporation of frequency resolved optical gating (FROG) [10], they are not capable to ensure complete space-time characterization of the resulting wave-packet. To date, few efforts in providing complete space-time characterization of ultrashort wave-packets had not been successful. An example has been that reported in [11]. The used technique, based on optical polarigraphy, has shown indeed a quite poor resolution, and did not allowed the fine details of the ST structure to be recovered.

Recent achievements in disclosing the phenomenology of the filamentation process have revealed that the wave-packet undergoes dramatic transformation from initial Gaussian towards final conical one, which resembles basic properties of the Bessel beam or the X-shaped wave [12]. In other words, the resulting wave packet acquires a complex shape, which can not be recovered by simple means. In a recent work related to the investigation of the nonlinear dynamics of X-waves in quadratic non-linear media some of the present authors have demonstrated a very powerful, high ST resolution 3D-mapping technique, based on the use of

ultrafast χ^2 gate [13, 14]. The approach resembled the crosscorrelation measurement to some extent, but instead of recording the space-integrated (or simply on-axis) signal, the entire space-time resolved sum-frequency (SF) intensity profile is captured.

By means of three dimensional imaging technique we studied experimentally the space-time transformation of a Gaussian wave-packet, which undergoes self-focusing in nonlinear medium. The nonlinear medium that we have chosen is water; with respect to solid-state media, it has the key advantages of being free from damage problems, and of allowing easy and continuous scanning of sample length; in comparison with air, water has much less turbulence, which results in higher beam-pointing stability.

2 Numerical model and simulations

The modelling of the ultrashort-pulse self-focusing dynamics in Kerr media is one of the most challenging physical and computational tasks in non-linear optics, which virtually requires the use of full Maxwell equations with plenty of non-linear terms. However, as it was demonstrated recently, the numerical model accounting only for diffraction, self-focusing and nonlinear losses is sufficient in describing spatial features of beam filamentation [15]. The distinctive feature of our model is that it completely neglects the alleged defocusing effect of the electron plasma created due to multi-photon ionization.

Specifically, we consider evolution of the a linearly polarized beam propagating with central frequency ω_0 and wave-number $k = \omega_0 n/c$. Here $n = 1.33$ is the linear refraction index of the water at propagation wavelength $\lambda = 527$ nm. Since we are going to concentrate on space-time effects and will not involve multi-filamentation effects [16] into consideration, the cylindric symmetry could be assumed. In this case complex scalar envelope $A(r, z, t)$ of the beam in the nonlinear medium (including diffraction, chromatic dispersion, self-focusing and nonlinear losses) evolves according the modified nonlinear Schrödinger equation. In the frame of the adopted paraxial approximation moving at the group velocity

$v_g = [\partial k(\omega)/\partial \omega]^{-1}$, the resulting equation for the field amplitude, A reads:

$$\begin{aligned} \frac{\partial A}{\partial z} = & \frac{ik''}{2} \frac{\partial^2 A}{\partial t^2} + \frac{ik'''}{3} \frac{\partial^3 A}{\partial t^3} + \frac{i}{2k} \left(\frac{\partial^2 A}{\partial r^2} + \frac{1}{r} \frac{\partial A}{\partial r} \right) \\ & + \frac{i\omega_0 n_2}{c} |A|^2 A - \frac{\beta^{(K)}}{2} |A|^{2K-2} A, \end{aligned} \quad (1)$$

where $k'' = \partial^2 k(\omega)/\partial \omega^2$ and $k''' = \partial^3 k(\omega)/\partial \omega^3$ are the second and third order dispersion coefficients, respectively, z is the propagation distance, n_2 is the nonlinear index of refraction defined as $\Delta n = n_2 I$, and $\beta^{(K)}$ is the multiphoton absorption coefficient.

The laser pulse profile at the entrance of the nonlinear media was taken in the form of Gaussian in space and tailored Gaussian in time:

$$A(r, \tau, 0) = \frac{A_0}{1+0.7e^{-1}} \exp\left(-\frac{r^2}{w_0^2}\right) \left[\exp\left(-\frac{t^2}{\tau^2}\right) + 0.7 \exp\left(-\frac{(t+\tau)^2}{\tau^2}\right) \right], \quad (2)$$

with initial beam waist $w_0 = 75 \mu\text{m}$, temporal half-width duration $\tau = 150 \text{ fs}$ and amplitude $A_0 = \sqrt{2P_0/\pi w_0^2}$, in agreement with experimental conditions as described below. P_0 here stands for input beam power at the pulse maximum. (Note, that non-symmetric initial pulse was taken initially, even if this circumstance does not play significant role in ruling the temporal dynamics.)

It is convenient to normalize beam power to its critical value for the self-focusing $P_{cr} = 3.77\lambda^2/(8\pi n n_2)$. In this case equation (1) reads:

$$\begin{aligned} \frac{\partial A}{\partial z} = & \frac{ik''}{2} \frac{\partial^2 A}{\partial t^2} + \frac{ik'''}{3} \frac{\partial^3 A}{\partial t^3} + \frac{i}{2k} \left(\frac{\partial^2 A}{\partial r^2} + \frac{1}{r} \frac{\partial A}{\partial r} \right) \\ & + i \frac{3.77\lambda}{2\pi n w_0^2} |A|^2 A - \widetilde{\beta^{(K)}} |A|^{2K-2} A, \end{aligned} \quad (3)$$

where, after normalization of the amplitude A to the critical one ($A_{cr} = \sqrt{2P_{cr}/\pi w_0^2}$), intensity dependent multi-photon absorption coefficient reads: $\widetilde{\beta^{(K)}} = \beta^{(K)} \times |A_{cr}|^{2K-1}$. In our calculations we took $k'' = 5.2 \times 10^{-4} \text{ ps}^2/\text{cm}$, $k''' = 2.8 \times 10^{-7} \text{ ps}^3/\text{cm}$ for material dispersion [17] and $\widetilde{\beta^{(K=4)}} = 0.00005 \text{ cm}^{-1}$ for nonlinear absorption coefficient. We assume that four-photon absorption ($K = 4$) takes place, considering the bandgap of water $E_g = 6.5 \text{ eV}$, photon energy of 2.3 eV and that additional photon is absorbed by photogenerated plasma [12].

The nonlinear differential equation (3) was solved numerically. We used a split-step procedure to separate the nonlinear equation into dispersive, diffractive and nonlinear parts, and solved them inside each step separately. A fast Fourier transform (FFT) to wave-numbers – frequency space was used for dispersive step. After an inverse transform back to space-time representation, the fourth order Runge-Kutta procedure was used to evaluate the nonlinear step, whereas finite difference method was used for the diffractive step.

Figure 1 shows the results of numerical simulations. Simulation reveals that high-power pulses undergo spatial transformations forming ring-like lateral structure and temporal compression, splitting and regeneration of the central spike at $t = 0$. This kind of spatio-temporal behavior persists within a wide range of input parameters, such as intensity and wavelength.

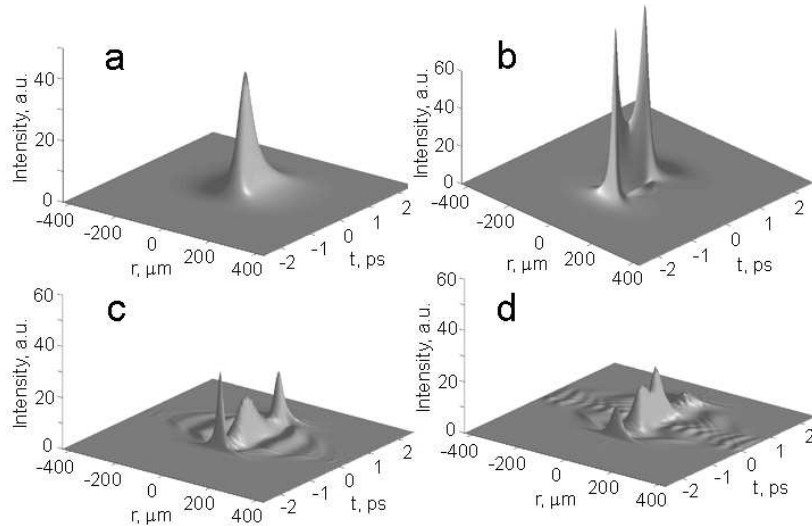


Fig. 1. Calculated space-time intensity profiles in the moving coordinate frame: (a) $z = 10$ mm; (b) 15 mm; (c) 25 mm; (d) 35 mm. Input pulse power: $P = 5P_{cr}$.

3 Experimental setup

The principle of three dimensional imaging technique was recently suggested and described in detail in [18]. Fig. 2 illustrates the basic idea of the method: for a

chosen delay time, short probe pulse interacts with a short temporal slice of the test wave-packet within the nonlinear crystal, and generates the sum-frequency (SF) signal. It's fluence profile is then imaged and recorded by a CCD camera. Then by spanning the delay time, the assembly of time slices is collected. The ST intensity map of the test wave-packet is then reconstructed with high temporal and spatial resolution being defined by the duration of the probe pulse.

The experimental layout consists of four different blocks: (i) the test (arbitrarily shaped) wave-packet generator; (ii) the probe pulse generator; (iii) nonlinear gate; (iv) data acquisition system.

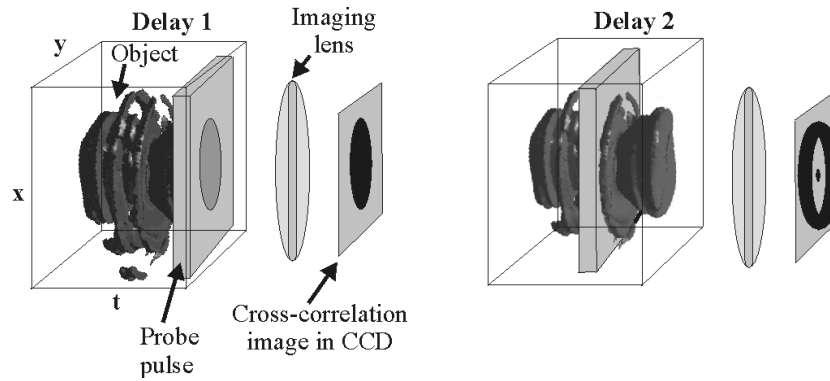


Fig. 2. Schematic representation of three dimensional imaging technique.

(i) The test (arbitrarily shaped) wave-packet was excited by launching spatially filtered and focused $0.9\text{-}\mu\text{J}$, 150-fs , 527-nm pulses into a syringe shaped water cell (using focusing geometry as described in [6]). The input pulses were generated by a frequency up-converted optical parametric amplifier (TOPAS, Light Conversion Ltd.), pumped by 100-fs , 800-nm pulses delivered by Ti:Sapphire laser system (Spitfire, Spectra Physics) at 1 kHz repetition rate. With input power 5 times above P_{cr} ($P_{cr} = 1.15\text{ MW}$ in water at $\lambda = 527\text{ nm}$ as derived from standard equation $P_{cr} = 3.77\lambda^2/8\pi n n_2$, $n_2 = 2.7 \times 10^{-16}\text{ cm}^2/\text{W}$), a single filament with white light spectrum content and FWHM diameter of $45\text{ }\mu\text{m}$ FWHM was excited.

(ii) High intensity contrast, 20-fs and $13\text{-}\mu\text{J}$ probe pulse with wavelength centered at 710 nm was provided by a non-collinear optical parametric ampli-

fier (TOPAS White, Light Conversion Ltd.) pumped by a frequency doubled Ti:Sapphire laser pulses and has 1 mm FWHM diameter.

(iii) Sum frequency mixing process between the test and the probe pulses in a thin ($20 \mu\text{m}$) type I phase-matching β -barium borate (BBO) crystal served as a nonlinear gate. In order to avoid severe distortions of the test pulse spatial profile imposed by free-space propagation, it has been imaged onto the input face of the nonlinear crystal by means of magnifying telescope. SF signal centered at 302 nm was then imaged onto the high dynamic range CCD camera. In this configuration, the field obtained via SF generation in BBO crystal results in a fluence distribution (x, y, t_1, z_0) at given delay t_1 . In order to obtain SF signal proportional to the object intensity, where z_0 corresponds to the fixed plane selected by the imaging telescope ($z_0 = 0$ at the water cell output-face plane), we employed a probe pulse with constant intensity over the area of the test wave-packet to be characterized (note 1 mm FWHM diameter), and ensured that SF process is performed in the low conversion limit. Then by spanning the delay t by motorized stepper motor (we use 12 fs steps), the complete intensity map $I(x, y, t, z_0)$ can be retrieved, the ultimate temporal resolution being defined by the probe pulse width, by its front steepness and by its intensity contrast. We note, that temporal, as well as spatial walk-off between the test and probe wave packets were negligible for such a thin crystal. The sequence of SF fluence profiles that correspond to different delay times is sketched in Fig. 3.

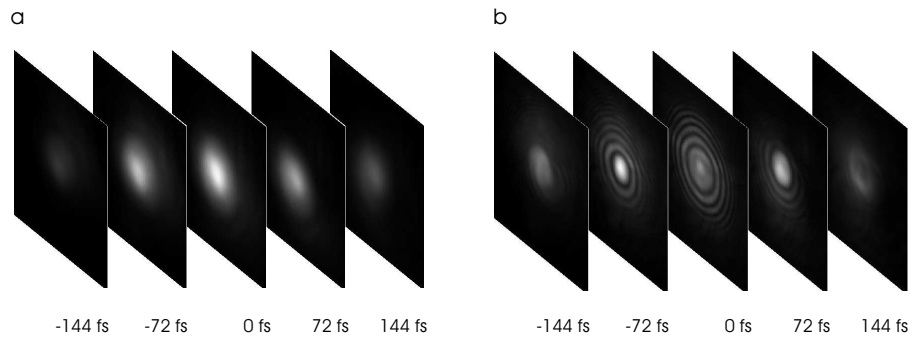


Fig. 3. Time resolved intensity profiles of the wave packet: (a) input Gaussian wave packet $I(x, y, t, z = 0 \text{ mm})$; (b) test wave packet after self-focusing $I(x, y, t, z = 22 \text{ mm})$. Negative and positive delay times denote the leading and the trailing edges of the pulse, respectively.

(iv) The acquisition was performed by imaging the output face of the BBO crystal onto a CCD detector (Andor Technology) and by acquiring the fluence profile of the SF signal for different time delay. The use of a high dynamic (16 bit/pixel), low noise (cooled down to -50°C) CCD with background subtraction allowed us to perform high sensitivity and high dynamic range detection, while keeping very low energy conversion in the SF process. Typically, CCD on-chip integration over 1000 shots was performed.

4 Experimental results

The main set of the results yielding complete characterization of the test wavepacket is depicted in Figs. 4–6. By means of time-integrated spatial detection, we measured a single filament of $\sim 45\ \mu\text{m}$ FWHM diameter, which is formed at $z = 15\ \text{mm}$, being surrounded by oscillating annular ring structure (Fig. 4). This

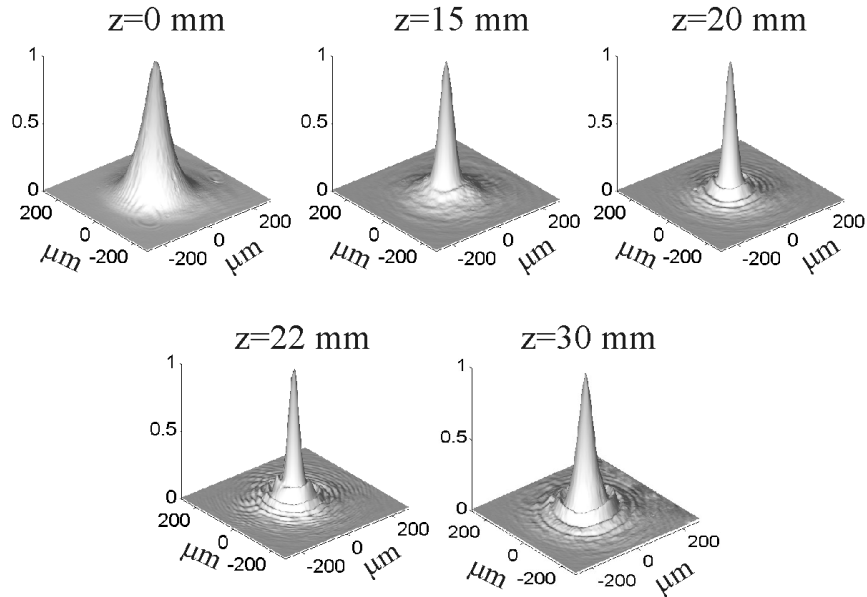


Fig. 4. Normalized time-integrated fluence profiles versus z of 150-fs pulse propagating in water at $P = 5P_{cr}$.

structure persists over the investigated z range, with slight changes in the diameter

of the central spike. Fig. 5 illustrates the spatio-temporal intensity profiles of the reconstructed wave packet at different z , as measured by changing length of the water cell. We note that the launched pulse has an asymmetric initial temporal profile (see space-time profile at $z = 0$ mm in Fig. 5) with a shoulder on its trailing

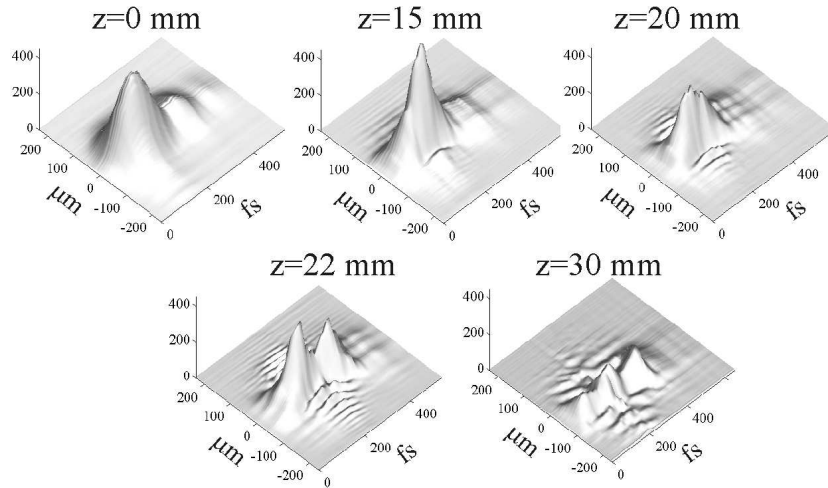


Fig. 5. Evolution of space-time intensity profiles versus z of 150-fs pulse propagating in water at $P = 5P_{cr}$.

edge. We expect that this shoulder, because of its low intensity, does not play any relevant role in the nonlinear dynamics. Fig. 6 shows the corresponding intermediate field angularly resolved frequency spectra at the vicinity of the carrier frequency recorded by means of imaging spectrometer.

The space-time maps show evident pulse compression at $z = 15$, on axis splitting at $z = 22$ mm, followed by the recombination at $z = 30$ mm. Out of the beam axis intense modulated wings appear, whose intensity remain peaked at the pulse central temporal coordinate. This last feature is particular important if one accounts that the major part of the wave-packet energy is indeed contained into the outer part of the beam. In fact, direct measurements by means of pinholes and stoppers had shown that the central spike (filament) contains less than 20% of the total energy [12]. These results let us foresee that pulse recombination could appear because of refocusing of a portion of a power distributed in these intense

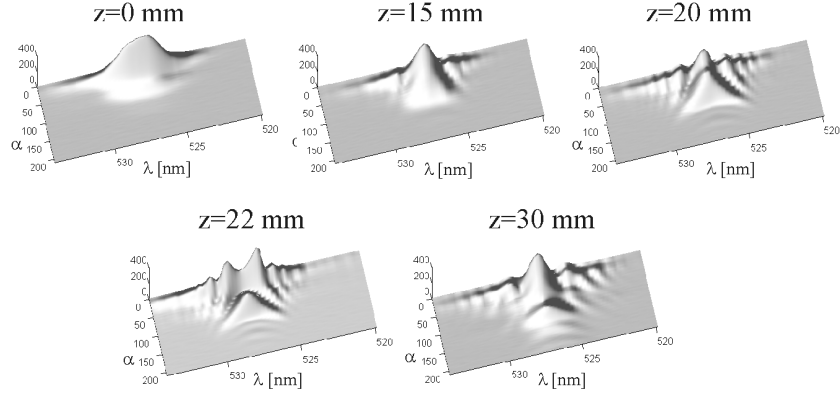


Fig. 6. Evolution of intermediate field frequency spectra recorded by means of imaging spectrometer.

outer rings. Deeper analysis shows that alleged pulse splitting, does not refer to entire wave packet, but just to very central portion of it, as power (space-integrated intensity) distribution remains peaked at the pulse center at any value of z [19].

For what concerns spectral measurements, the most impressive result is the strict similarity of intermediate field spectral distributions with space-time intensity maps. To this end, we note beside oscillating wings at the central frequency, the frequency splitting at $z = 22$ mm followed by recombination at $z = 30$ mm. Also we note clearly seen the X-type structure.

Recent data on filamentation dynamics of 150-fs pulse at 800 nm has fully confirmed our preliminary observations of complex dynamics, and, most importantly, the recombination of the central peak in time. To our opinion, these findings provide an indication of the fact that the wave packet is attempting a reshaping toward a supported eigenmode of the system, with either dominant Bessel type or X-type profile, owing to the interplay among self-focusing, dispersion and nonlinear losses [12, 20, 21].

5 Conclusions

In conclusion, we present high-resolution, high dynamic range detection system for quantitative space-time recovery of complex wave-packets. The developed technique can be readily applied for characterization of arbitrarily shaped wave-

packets, transformed via space-time dynamics in various nonlinear media. As an example, we have investigated self-focusing of 150-fs Gaussian wave-packet in water. Our preliminary results point to complex space-time dynamics, which is ruled mainly by the interplay between self-focusing, chromatic dispersion and nonlinear losses. Observed pulse splitting and recombination of intense ultra-short pulses characterize just on-axis temporal intensity profile, but not the wave-packet as a whole. These effects seem to occur in conjunction with relevant energy exchange between the beam center and the self-built, slowly decaying, oscillating tails. We also note a good agreement between the experiment and numerical simulations.

Acknowledgement

The authors acknowledge valuable contribution of G. Tamošauskas, A. Varanavičius, J. Trull and A. Piskarskas and the support from MIUR (Cofin01/FIRB01) and EC CEBIOLA (ICA1-CT-2000-70027) contracts.

References

1. Bergé L. “Wave collapse in physics”, *Phys. Rep.*, **303**, p. 259-370, 1998
2. Braun A., Korn G., Liu X., Du D., Squier J., Mourou G. “Self-channeling of high-peak-power femtosecond laser pulses in air”, *Opt. Lett.*, **20**, p. 73–75, 1995
3. Mlejnek M., Wright E.M., Moloney J.V. “Femtosecond pulse propagation in argon: A pressure dependence study”, *Phys. Rev. E*, **58**, p. 4903–4909, 1998
4. Couairon A., Tzortzakis S., Bergé L., Franco M., Prade B., Mysyrowicz A. “Infrared femtosecond light filaments in air: simulations and experiments”, *J. Opt. Soc. Am. B*, **19**, p. 1117–1131, 2002
5. Tzortzakis S., Sudrie L., Franco M., Prade B., Mysyrowicz A., Couairon A., Bergé L. “Self-guided propagation of ultrashort IR laser pulses in fused silica”, *Phys. Rev. Lett.*, **87**, 213902, 2001
6. Dubietis A., Tamošauskas G., Diomin I., Varanavičius A. “Self-guided propagation of femtosecond light pulses in water”, *Opt. Lett.*, **28**, p. 1269–1271, 2003
7. Liu W., Chin S. L., Kosareva O., Golubtsov I.S., Kandidov V.P. “Multiple refocusing of a femtosecond laser pulse in a dispersive liquid (methanol)”, *Opt. Commun.*, **225**, p. 193–209, 2003

8. Chin S.L., Brodeur A., Petit S., Kosareva O.G., Kandidov V.P. “Filamentation and supercontinuum generation during the propagation of powerful ultrashort laser pulses in optical media (White Light Laser)”, *J. Nonlinear Opt. Phys. Mater.*, **8**, p. 121–146, 1999
9. Gaeta A.L. “Catastrophic collapse of ultrashort pulses”, *Phys. Rev. Lett.*, **84**, p. 3582–3585, 2000
10. Bernstein A.C., Diels J.-C., Luk T.S., Nelson T.R., McPherson A. Cameron S.M. “Time-resolved measurements of self-focusing pulses in air”, *Opt. Lett.*, **28**, p. 2354–2356, 2003
11. Kumagai H., Cho S.-H., Ishikawa K., Midorikawa K., Fujimoto M., Aoshima S., Tsuchiya Y. “Observation of the complex propagation of a femtosecond laser pulse in a dispersive transparent bulk material”, *J. Opt. Soc. Am. B*, **20**, p. 597–604, 2003
12. Dubietis A., Gaižauskas E., Tamošauskas G., Di Trapani P. “Light filaments without self-channelling”, *Phys. Rev. Lett.*, **92**, 253903, 2004
13. Di Trapani P., Valiulis G., Piskarskas A., Jedrkiewicz O., Trull J., Conti C., Trillo S. “Spontaneously Generated X-Shaped Light Bullets”, *Phys. Rev. Lett.*, **91**, 093904, 2003
14. Trull J., Jedrkiewicz O., Di Trapani P., Matijošius A., Varanavičius A., Valiulis G., Danielius R., Kučinskas E., Piskarskas A., Trillo S. “Spatio-temporal 3D mapping of nonlinear X-waves”, *Phys. Rev. E*, **69**, 026607, 2004
15. Dubietis A., Kučinskas E., Gaižauskas E., Tamošauskas G., Di Trapani P. “Formation dynamics of light filaments in water”, *Lithuanian J. Phys.*, **43**, p. 437–442, 2003
16. Dubietis A., Tamošauskas G., Fibich, G. Ilan, B. “Multiple filamentation induced by input-beam ellipticity”, *Opt. Lett.*, **29**, p. 1126–1128, 2004
17. Van Engen A.G., Diddams S.A., Clement T.S. “Dispersion measurements of water with white-light interferometry”, *Appl. Opt.*, **37**, p. 5679–5686, 1998
18. Potenza M.A.C., Minardi S., Trull J., Blassi G., Salerno D., Varanavičius A., Piskarskas A. Di Trapani P. “Three dimensional imaging of short pulses”, *Opt. Commun.*, **229**, p. 381–390, 2004
19. Matijošius A., Trull J., Di Trapani P., Dubietis A., Piskarskas R., Varanavičius A., Piskarskas A. “Non-linear space-time dynamics of ultrashort wave packets in water”, *Opt. Lett.*, **29**, p. 1123–1125, 2004
20. Porras M.A., Parola A., Dubietis A., Di Trapani P. “Stationary conical waves supported by nonlinear absorption”, *Phys. Rev. Lett.* (submitted)
21. Kolesik M., Wright E.M., Moloney J.V. “Dynamic nonlinear X-waves for femtosecond pulse propagation in water”, *Phys. Rev. Lett.*, **92**, 253901, 2004